Communications in Computational Chemistry
Commun. Comput. Chem., Vol. 1, No. 2, 161–170
doi: 10.4208/cicc.2025.99.01
Regular Article

Energy Near-Degeneracy Driven Covalency Analyzed by a Two-Electron Two-Orbital Model

Michael Dolg[1,2,*]

[1] *Key Laboratory of Theoretical and Computational Photochemistry, College of Chemistry, Beijing Normal University, Beijing 100875, China;*

[2] *Theoretical Chemistry, University of Cologne, 50939 Cologne, Germany.*

[*] Corresponding author: Michael Dolg m.dolg@bnu.edu.cn; m.dolg@uni-koeln.de

Received on 9 April 2025; Accepted on 25 April 2025

Abstract: A simple model based on the two-electron two-orbital textbook problem is presented and used to analyze pairwise interatomic interactions in metal-ligand bonding. In particular the two types of covalency discussed during the last decade for actinide-ligand interactions, overlap/interaction driven and energy-near-degeneracy driven covalency, as well as their influence on the bond strengths and interatomic charge build-up are discussed. The hydration complexes $M(H_2O)_n^{4+}$ of selected tetravalent lanthanide and actinide ions are used to probe the performance of the model for an analysis of calculations as well as for predictions.

Key words: bonding, covalency, actinides, lanthanides.

1. Introduction

The involvement of actinide 5f orbitals in chemical bonding was already discussed as early as 1954 by Seaborg and coworkers [1] and has been a hotly debated topic of numerous research articles since then, which are summarized in several reviews [2-15]. Actinide-ligand bonding is a very complicated topic, due to the influence of many factors such as relativistic and correlation effects, numerous low-lying electronic states on the actinide center in case of open 5f shells, the changing character of the 5f shell from initially diffuse Rydberg type in Fr and Ra, over valence-type to rather core-like along the actinide row, as well as a competitive participation in bonding of 5f, 6d, 7p and 7s orbitals with different abilities or preferences for ionic and covalent interactions. In so far it is somewhat surprising that simple ideas from molecular orbital theory still are able to offer some insight.

Recently two concepts to explain reasons for covalent bonding in actinide complexes have been proposed [16] and extensively used [17-25], i.e., orbital overlap or interaction driven and energy (near-)degeneracy driven covalency. Following the original article of Neidig et al. [16] these types of covalency can be briefly explained as follows. The theoretical foundation is a perturbative approach of MO-LCAO (molecular orbitals by linear combination of atomic orbitals) theory to actinide-ligand bonding, starting with an ionic picture of a complex, i.e., $M^{n+}(L^{m-})_k$, as zeroth order. A metal orbital ϕ_M with orbital energy ϵ_M, and a ligand orbital ϕ_L with orbital energy ϵ_L, can mix leading to an antibonding

$$\varphi_a = \frac{1}{\sqrt{1 + 2\lambda S_{ML} + \lambda^2}}(\phi_M + \lambda\phi_L) \qquad (1)$$

and a bonding

$$\varphi_b = \frac{1}{\sqrt{1 - 2\lambda S_{ML} + \lambda^2}}(\phi_L - \lambda\phi_M) \qquad (2)$$

linear combination, with S_{LM} being the overlap integral between ϕ_M and ϕ_L. We note that, probably due to their intention to analyze, e.g., K-edge X-ray absorption spectroscopy (XAS) results, the authors focus on the antibonding, in the ground state unoccupied linear combination φ_a with a leading metal contribution ($\lambda \leq 0$). In the core excited states probed by spectroscopy this orbital becomes occupied and its An 5f contributions are related to spectroscopic features. In a two-orbital model orthogonality then determines the bonding orbital φ_b occupied in the ground state and thus allows to calculate An 5f contributions. Using these ideas An 5f covalency in the ground state can be experimentally 'measured'. However, some problems might arise since the unoccupied orbital probed by XAS is probably best described as a canonical orbital, whereas for bonding discussions localized occupied orbitals are more appropriate.

The mixing coefficient λ is given by first-order perturbation theory as

$$\lambda = \frac{H_{ML}}{\epsilon_M - \epsilon_L} \qquad (3).$$

Note that $\epsilon_M > \epsilon_L$ and $H_{ML} \leq 0$ leads to $\lambda \leq 0$, i.e., the antibonding and bonding linear combinations in eqns. 1 and 2, respectively. According to the Wolfsberg-Helmholz model the Hamiltonian matrix element H_{ML} is proportional to the overlap integral S_{ML} [26]. A parameter $\lambda = 0$ results in the ionic case without orbital mixing, i.e., an unoccupied metal orbital $\varphi_a = \phi_M$ and an occupied ligand orbital $\varphi_b = \phi_L$, whereas $\lambda = -1$ corresponds to the antibonding $\varphi_a \sim \phi_M - \phi_L$ and bonding $\varphi_b \sim \phi_L + \phi_M$ linear combinations of a homonuclear diatomic such as H_2. As noted by Neidig et al. [16] a corresponding two-electron covalent bond has still 50% ionic and 50% covalent contributions, as becomes obvious from expanding the delocalized orbital product for the bonding orbital $\varphi_b \sim \phi_M + \phi_L$ into two ionic and two covalent terms with localized orbitals

$$\varphi_b(1)\varphi_b(2) \sim \phi_L(1)\phi_L(2) + \phi_M(1)\phi_M(2) + \phi_L(1)\phi_M(2)$$

$$+ \phi_M(1)\phi_L(2) \qquad (4).$$

It was argued that according to eqn. 3 covalent interactions may be realized in two ways:

- a large (absolute value of the) Hamiltonian matrix element H_{ML} in the numerator, i.e., a large overlap matrix element S_{ML}, which is thus refered to as overlap driven covalency, or
- a vanishing denominator $\epsilon_M - \epsilon_L$, which is denoted as near degeneracy driven covalency.

The 'traditional' idea of covalent bonding in chemistry is that the interaction leads to orbital mixing and as a consequence to a buildup of charge between the atoms, at the same time leading to a stabilization of the bonding orbital, whereas in the physical community a mixing of atomic orbitals in canonical molecular orbitals is often considered as covalency. Neidig et al. [16] point out that the charge buildup between the metal atom and the ligand depends on the type of covalency. Near-degeneracy driven covalency may result in orbital delocalization and not necessarily a large charge redistribution. Moreover, orbital mixing termed as covalency by the physics community does not need to be accompanied by stronger bonds as expected for covalency in the chemistry community, since the energy associated with covalent mixing in second-order perturbation theory is given as

$$\Delta E = \frac{|H_{ML}|^2}{\epsilon_M - \epsilon_L} = \lambda H_{ML} \qquad (5).$$

Two bonds with the same mixing coefficient λ may have different covalent contributions to the bonding energy depending on the Hamiltonian matrix element H_{ML}. Finally, Neidig et al. [16] remarked that both types of covalency may be operative for different classes of complexes, depending on the ligand and the metal oxidation state.

It has to be mentioned that recently Sergentu and Autschbach criticized the usage of the concept of energy-driven covalency, or orbital mixing without overlap, applied previously for the interpretation of K-edge X-ray absorption near edge structure (XANES) spectra of $AnCl_6^{2-}$ (An=Th-Pu) complexes [23] in contrast to the conventional covalency based on overlap and orbital mixing as unnecessary [27]. Recent related work analyzes the covalency in CeX_6^{2-} complexes [28]. In an earlier article they in addition emphasized that, as shown by relativistic multi-configurational ab initio calculations, actinide-ligand covalency in core excited states such as probed by XANES spectroscopy may be different from the covalency in the ground state [29].

In the following we use the ideas of Neidig et al. [16] as a starting point for a related minimalistic model, which is based on a variational rather than a perturbative approach for a two-electron two-orbital bond [30]. Schwarz and collaborators discussed the covalent binding energy contributions in lanthanide trihalides molecules in terms of such a model [31]. They emphasize that the covalent bond stabilization is limited by $2H_{ML}$, i.e., there is no covalency in the sense of a bond stabilization without a metal-ligand interaction $H_{ML} \neq 0$. In addition, a nonvanishing positive bond order can result for orbital mixing without interaction, i.e., for a vanishing bond stabilization. As for the model of Neidig et al. [16] the focus of the present work is only on metal-ligand bonding, i.e., bonding between two centers, a positively charged metal ion with (partially) unoccupied valence orbitals and a ligand atom able to donate electron density into these. By no means it is intended to establish an universally applicable approach to analyze other bonding situations, such as, e.g., multiple-center covalent bonding, metallic bonding, van der Waals bonding, etc..

Kaltsoyannis, Dognon, Kerridge and other experts in the field actually strongly advocate analytic approaches which do not rely on the sometimes not uniquely defined orbitals, but rather on observables as the electron density [10, 11, 13, 15], e.g., the quantum theory of atoms in molecules (QTAIM) by Bader [32]. In fact multi-configurational treatments combined with subsequent orbital localization might result for many cases in orbital sets which are more useful for interpretation than commonly used single-reference based approaches such as density functional theory (DFT), and remove signs of 'interactions' which are rather due to the restriction to one configuration than to physical interactions. For example, it is well known that treating H_2 $^1\Sigma_g^+$ at large distance with both the $\varphi_b^2 = \sigma_g^2$ bonding and $\varphi_a^2 = \sigma_u^2$ antibonding configurations allows to form a $\varphi_b^2 - \varphi_a^2$ linear combination and thus to remove the ionic terms mentioned above from the wavefunction. After orbital localization one can write the resulting spatial wavefunction in terms of the contributing atomic orbitals $\phi_L = 1s_A$ and $\phi_M = 1s_B$, i.e., $\phi_L(1)\phi_M(2) + \phi_M(1)\phi_L(2)$, which reflects much more correctly the picture of two noninteracting neutral H atoms in their $1s^1$ ^2S ground states. We also note that it was found by Kaltsoyannis that (sometimes) different tools yield different conclusions [9], and probably for this reason Dognon recommended always to use various complementary tools for analysis of actinide-ligand bonding [10]. Nevertheless, sticking despite its limitations deliberately to a single configuration approach and to orbitals, which are familiar to and popular among chemists, it is hoped that results obtained with such a low-level model bring easily to remember insight in the terms overlap/interaction driven and energy (near-)degeneracy driven covalency. Finally we want to point out that when digging deeper even ordinary covalency for systems such as H_2 is by no means a simple topic [33].

2. Theoretical method

We start, as in most textbooks, with two real, normalized and for reasons of simplicity orthogonal orbitals ϕ_L and ϕ_M, localized on a ligand atom (L) and a metal ion (M), respectively. Inclusion of a non-zero overlap is possible, but it complicates the matter and does not lead to entirely different conclusions [30]. Unless otherwise noted we assume that two electrons with opposite spin occupy as a pair the energetically lowest orbital, e.g., for an ionic system M^+L^- the ligand orbital, or for a polar system the bonding linear combination of metal and ligand orbitals. We further introduce the three parameters $\Delta = F_{MM} - F_{LL} \geq 0$, $\Sigma = F_{MM} + F_{LL} \leq 0$ and $v = F_{LM} = F_{ML} \leq 0$ in terms of the elements of corresponding two-by-two Fock matrix **F**. Note that Δ is the energy gain when forming a pure ionic bond, whereas $2|v|$ is the energy gain for a pure covalent bond. The associated matrix eigenvalue problem

$$\mathbf{Fc} = \varepsilon\mathbf{c} \qquad (6)$$

leads to the eigenvalues

$$\epsilon_{1,2} = \frac{\Sigma \mp \sqrt{\Delta^2 + 4v^2}}{2} \qquad (7)$$

The splitting of the eigenvalues $\epsilon_1 \leq \epsilon_2$ can be written as a sum of an ionic and a covalent contribution

$$\Delta\epsilon = \epsilon_2 - \epsilon_1 = \Delta\epsilon_{ion} + \Delta\epsilon_{cov}$$

$$= \Delta + \left[\sqrt{\Delta^2 + 4v^2} - \Delta\right] \qquad (8).$$

Ionic limit: M^+L^- $v = 0, \Delta \neq 0 \Rightarrow \Delta\epsilon = \Delta$ Small covalency: $v \neq 0$ $\lvert v\rvert << \Delta \Rightarrow \Delta\epsilon \approx \Delta + 2\frac{v^2}{\Delta}$	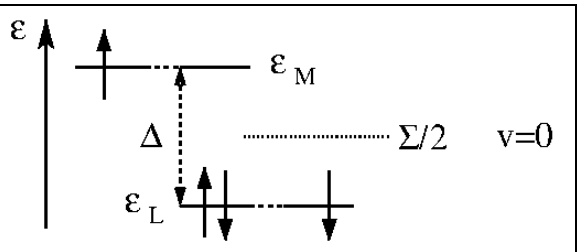
Covalent limit: M L $\Delta = 0, v \neq 0 \Rightarrow \Delta\epsilon = 2\lvert v\rvert$ Small ionicity: $\Delta \neq 0$ $\Delta << \lvert v\rvert \Rightarrow \Delta\epsilon \approx 2\lvert v\rvert + \frac{1}{4}\frac{\Delta^2}{\lvert v\rvert}$	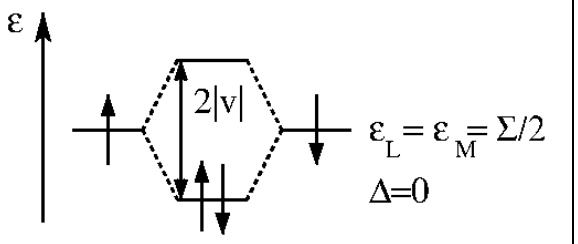

Figure 1. Limiting cases of ionic and covalent bonding.

Binding energy: $\Delta E = \Delta E_{ion} + \Delta E_{cov} = \sqrt{\Delta^2 + 4v^2}$ Ionic contribution: $\Delta E_{ion} = \Delta$ Covalent contribution: $\Delta E_{cov} = \sqrt{\Delta^2 + 4v^2} - \Delta$	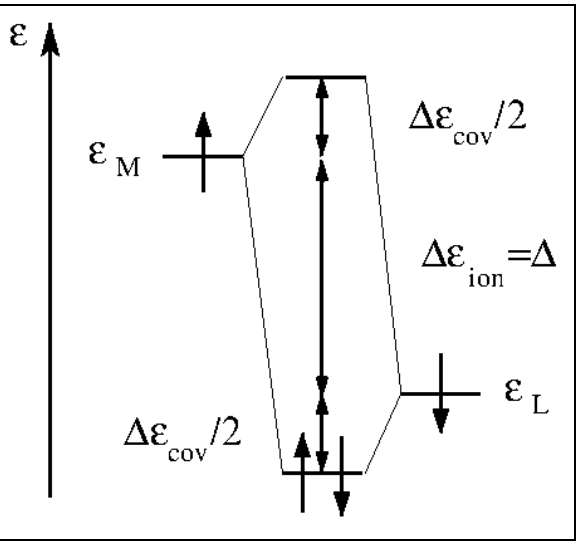

Figure 2. Polar bonding.

The molecular orbital (MO) schemes corresponding to the well-known limiting ionic (v=0) and covalent (Δ=0) cases, as well as the increases of the orbital energy splittings $\Delta\epsilon$ obtained by Taylor expansions for small covalency $|v| << \Delta$ and small ionicity $\Delta << |v|$ are given in Figure 1. It is obvious from eqn. 7 as well as eqn. 8 that the absence of an interaction ($v = 0$) does not lead to any changes of the atomic energies $\epsilon_1 = H_{LL}$ and $\epsilon_2 = H_{MM}$, i.e., covalency in the sense of a bonding contribution between two centers requires an interaction ($|v| > 0$). In case of an additional vanishing splitting Δ of the atomic levels the eigenvalues $\epsilon_{1,2}$ coincide and arbitrary linear combinations of ϕ_M and ϕ_L solve the Fock equation. Such an orbital mixing is not a covalency in the usual sense of chemistry.

We now consider a polar bond formed by two electrons and calculate from the orbital energy changes the total binding energy

$$\Delta E = \sqrt{\Delta^2 + 4v^2} \qquad (9).$$

Again, this quantity can be split into an ionic and a covalent term. The results are summarized in Figure 2.

One can now form the ratio of covalent and ionic contributions to the binding energy, which is a function of the parameter ratio $|v|/\Delta$,

$$\frac{\Delta E_{cov}}{\Delta E_{ion}} = \sqrt{1 + 4\frac{v^2}{\Delta^2}} - 1 \qquad (10).$$

For a subsequent discussion of the influence of changes in metal or ligand contributions to the bond strength we write two alternative expressions and their corresponding Taylor expansions for the binding energy,

$$\Delta E = \Delta\sqrt{1 + 4\frac{v^2}{\Delta^2}} \approx \Delta + 2\frac{v^2}{\Delta}$$

for $|v| << \Delta$ (case 1) (11)

and

$$\Delta E = |v|\sqrt{\frac{\Delta^2}{v^2} + 4} \approx 2|v| + \frac{1}{4}\frac{\Delta^2}{|v|}$$

for $\Delta << |v|$ (case 2) (12).

Assuming a polar bond with a relatively weak interaction ($|\Delta| \approx const. >> |v|$, case 1) one can see that an increase of the interaction $|v|$ leads to larger percentage of covalency (eqn. 10) and to a stronger bonding (eqn. 11), cf. Figure 3. In case of a polar bond with a relatively strong interaction ($|v| \approx const. >> \Delta$, case 2) one finds for an increasing degeneracy Δ also a larger percentage of covalency (eqn. 10), but a weaker bonding (eqn. 12), cf. Figure 4.

One can now look at the orbital coefficients for the bonding orbital and express the one for the metal orbital c_M as a function of the one on the ligand orbital c_L,

$$c_M = \frac{\Delta - \sqrt{\Delta^2 + 4v^2}}{2v} c_L \qquad (13).$$

For an ionic bond ($\Delta \to \infty$) one obtains for $c_L = 1$ a vanishing metal contribution $c_M = 0$. For a covalent bond ($\Delta = 0$) one gets $c_M = c_L$, where it has to be considered that $v < 0$ holds. For polar bonds one can write two Taylor expansions, i.e., for the case close to the ionic limit (large Δ)

$$c_M \approx \frac{|v|}{\Delta} c_L \qquad \text{for} \quad |v| << \Delta \quad \text{case 1} \qquad (14),$$

and the case close to the covalent limit (small Δ)

$$c_M \approx \left(1 - \frac{\Delta}{2|v|}\right) c_L \qquad \text{for} \quad \Delta << |v| \quad \text{case 2} \qquad (15).$$

In all cases, as obvious from the formulas above, there is no covalency in the sense of a bonding interaction for $v = 0$. Covalency requires an interaction between the two bonding partners, e.g., 'covalent bonding driven purely by energy degeneracy' or 'non-classical covalency' [14] does not exist, unless one counts orbital mixing due to degeneracy between non-interacting centers as covalency. Although these terms are embedded in an otherwise correct description of the situation, they bear the danger to be misunderstood in the sense that there might be another mechanism of covalency stabilizing a bond but not requiring interaction.

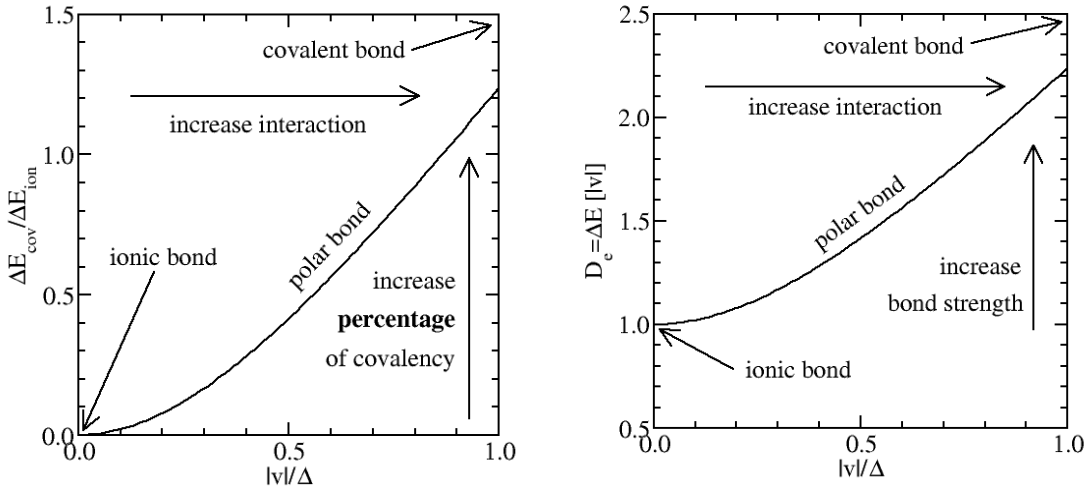

Figure 3. Case 1. Increasing the interaction increases the bond strength.

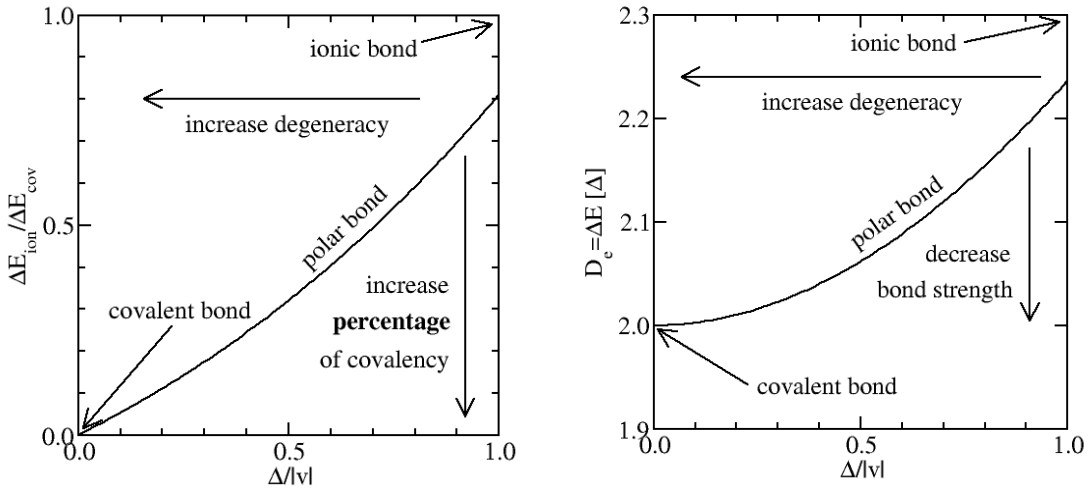

Figure 4. Case 2. Increasing the degeneracy decreases the bond strength.

As one can see from the formulas above the parameter $|v|/\Delta$ determines the mixing of the orbitals as well as the energy gain upon bonding. An interatomic charge build-up can be related to the product $c_L c_M$ of the orbital coefficients. Monitoring the change of $c_L c_M$ together with the one of the binding energy ΔE when going for a fixed value of the interaction $|v|$ from an ionic ($\Delta \to \infty$) to a covalent ($\Delta = 0$) bond one gets a monotonous increase of $c_L c_M$ together with a monotonous decrease of ΔE (energy (near-)degeneracy driven *increase* of covalency). Keeping the energy gap Δ constant and increasing the interaction $|v|$ monotonously increases the binding energy ΔE as well as the charge build-up measured by $c_L c_M$ (interaction driven *increase* of covalency). The dependence of the binding energy ΔE and the charge build-up $c_L c_M$ on $|v|$ and Δ is visualized in Figure 5. The cases 1 and 2 discussed above and depicted in Figures 3 and 4, respectively, are represented by the isolines for Δ and $|v|$. For example, substituting in a chelating ligand, e.g., 'hard' O by 'soft' S in order to increase the selectivity for 'soft' An^{n+} ion extraction over 'hard' Ln^{n+} extraction, decreases Δ and reduces the thermodynamic stability of the complexes (follow a $|v|$ isoline), unless the change also leads to a stronger metal-ligand interaction $|v|$ (change the $|v|$ isoline), e.g., due to spatially more extended ligand valence orbitals, for which the thermodynamic stability then in sum may be increased.

One may now ask where the regions for energy (near-)degeneracy driven and overlap/interaction driven covalency are located. It should be clear from the above described monotonous changes of ΔE and $c_L c_M$ as functions of $|v|$ and Δ and from Figure 5 that one cannot discern regions of special types of covalency. The limiting cases of ionic bonding ($\Delta > |v| = 0$) and covalent bonding ($|v| > \Delta = 0$) can easily be located on the lower and upper horizontal axis, respectively. They have no respectively a large interatomic charge build-up, and a binding energy depending on the energy gap Δ and the interaction $|v|$, respectively. Energy (near-)degeneracy driven covalency according to its inventors is associated with a small interatomic charge build-up and a low value of Δ, i.e., it should be located in the lower left corner of Figure 5. This region has no clear boundaries and is only accessible for small values of the interaction $|v|$. The associated energy gain ΔE is quite small. Thus it is a weak ionic interaction (if any) with only small covalent contributions. The $|v|/\Delta$ values are typically much smaller than 1, as can be easily seen for the crossing points of the isolines for $|v|$ and Δ. Our conclusion that energy (near-)degeneracy driven covalency is just a variant of ordinary covalency is in line with recent work of Sergentu and Autschbach, who based their similar conclusion on high level relativistic multi-reference ab initio studies of the XANES spectra of some protoype systems for energy (near-)degeneracy driven covalency [23], i.e., $AnCl_6^{2-}$ complexes [27].

The perturbation theory based argument mentioned in the introduction that for a decreasing value of Δ covalency is increased has to be viewed with some caution: decreasing Δ increases the interatomic charge build-up and weakens the bonding (e.g. follow the $|v| = 0.01$ curve in Figure 5), whereas energy (near-)degeneracy driven covalency is usually associated in literature with a small interatomic charge build-up. It also has to be noted that $c_L c_M$ is only useful as a relative measure of the interatomic charge build-up since it does not take into account the distance between the atoms. In the limit of a large interatomic distance, zero interaction and zero energy gap there is no energy gain and no interatomic charge build-up, although any value of $c_L c_M$ on the ΔE axis is possible since arbitrary linear combinations of ligand and metal orbitals solve the Fock equation.

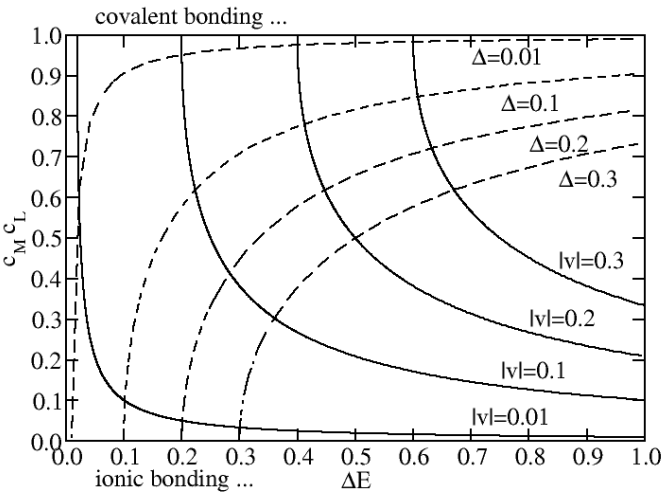

Figure 5. Charge build-up in the bonding region measured by the product of coefficients $c_L c_M$ vs. binding energy ΔE.

The usual type of covalency, the overlap/interaction driven covalency, is found at the top of Figure 5. Increasing the interaction $|v|$ increases the binding energy ΔE. For a fixed interaction $|v|$ an increase of Δ adds ionic bonding contributions and increases ΔE of the resulting polar covalent bond further. This is accompanied by a reduction of the interatomic charge build-up.

In a combined experimental and theoretical study of the XANES spectra of actinyl ions AnO_2^{2+} (An=U-Pu) it was stated, e.g., that the overlap-driven covalent character of the An-O binding decreases within the series U-Pu, 'while the energy-driven covalent character increases without increasing the electron density of the binding' and that 'energy-driven covalency might have a higher impact on chemical binding stability/strength than the overlap driven covalency' [22]. In view of Figure 5 such statements are questionable, i.e., increasing the orbital degeneracy without increasing the interatomic charge build-up (i.e., moving parallel to the ΔE axis from right to left), decreases the interaction $|v|$ (cf. crossing of $|v|$ isolines) as correctly stated, but of course strongly reduces the bond strength ΔE and ultimately leads to a vanishing impact on chemical binding stability/strength.

As will be shown below the pairwise interactions between the various metal and ligand orbitals may be associated with values for Δ and $|v|$ and each pair occupies a point in Figure 5. The ensemble of these interactions, which might have different ionic and covalent character, determines the overall complex stability.

3. Application

Finally it remains to be shown that the applied model is able to describe chemical bonding ranging between the limiting ionic and covalent cases for 'real' molecules, including actinide complexes. The model can be used in two ways, i.e., an 'analytic' mode trying to extract $|v|/\Delta$ from actual quantum chemical calculations on complexes, or a 'predictive' mode trying to get the parameters $|v|$ and Δ from calculations of the fragments prior to performing the calculation of the complex. The 'predictive' mode was already used in a previous publication [30].

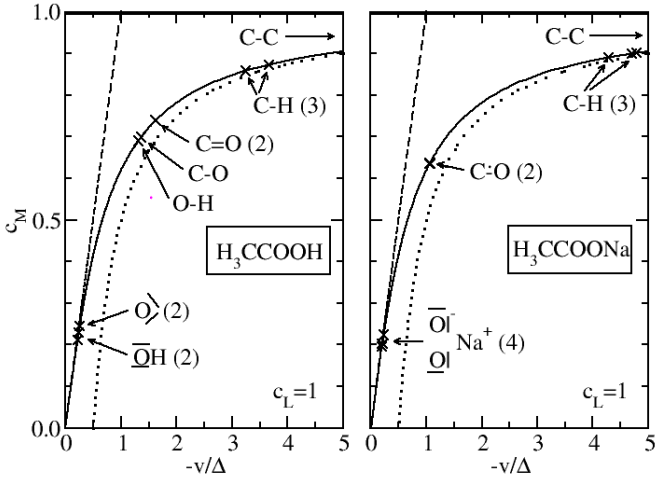

Figure 6. Covalency of bonds of the acetic acid molecule and the sodium acetate molecule in terms of |v|/Δ. The dashed straight line is the limiting expression for an ionic bond (eqn. 14), whereas the dotted curve corresponds to the covalent limit (eqn. 15).

For the analytic application we perform a Hartree-Fock (HF) or alternatively Kohn-Sham (KS) density functional theory (DFT) calculation using the TURBOMOLE program package [34, 35], apply a Foster-Boys localization of the orbitals and map those with predominant two-center contributions by means of the Mulliken populations to our two-electron two-orbital model. Core orbitals on the metal or ligand are excluded by means of a suitable orbital energy threshold. From the remaining valence orbitals only those are considered which have more of their electron density than a certain threshold, e.g. 1%, located on the metal atom, and a major contribution on the coordinating ligand atom. Small contributions on neighboring atoms are added to those of the coordinating ligand atom for simplicity. The normalized coefficient of the metal orbital c_M can then be simply determined from the Mulliken orbital population on the metal q_M by $2c_M^2 = q_M$. We note again that the aim is to describe metal-ligand interactions which can be reduced to pairs of contributing atoms and not more complicated types of bonding.

As an example not limited to actinide-ligand bonding we look at the acetic acid molecule and the sodium acetate molecule, where the full range of bonding from ionic to covalent is covered (Figures 6 and 7). It can be seen that the parameters $|v|/\Delta$ as well as $\Delta/|v|$ can well distinguish between bonds with different degrees of covalent and ionic interactions, completely in line with the expectations of a chemist. The proximity to the limiting curves allows to distinguish quantitatively between ionic, covalent, and polar bonding. When looking as in the following, at largely ionic metal-ligand interactions the representation using the parameter $|v|/\Delta$ is more appropriate.

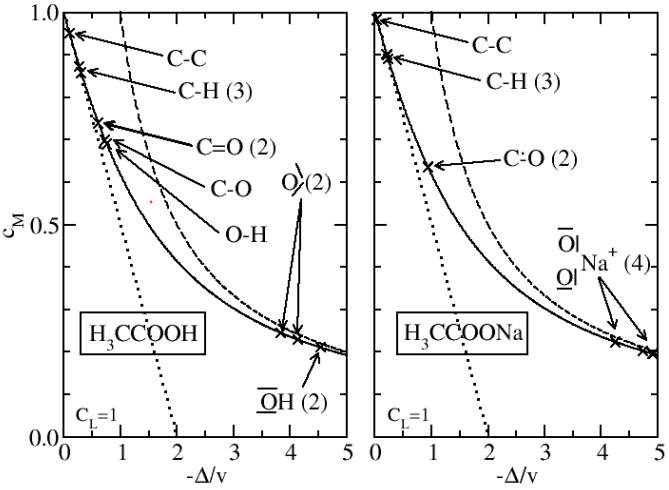

Figure 7. Covalency of bonds of the acetic acid molecule and the sodium acetate molecule in terms of Δ/|v|. The dashed curve is the limiting expression for an ionic bond (eqn. 14), whereas the dotted straight line corresponds to the covalent limit (eqn. 15).

From f-element chemistry we first look at the simple model systems $M(H_2X)^{4+}$ (M = Ce, Th; X = O, S), where the two lone pairs on X can donate electron density to the metal ion. HF calculations using relativistic pseudopotentials for the metals [36, 37] and basis sets of quadruple-zeta quality [38, 39] were performed. For the planar $M(H_2O)^{4+}$ systems there are two equal M-OH_2 interactions yielding $|v|/\Delta$ values of 0.42 for Ce and 0.33 for Th. The higher covalency of the Th system is confirmed, e.g., by the Wiberg bond orders [40] of 0.84 for Ce and 0.61 for Th. If the Wiberg bond order is derived from the model calculations instead of the full HF calculation values of 0.88 for Ce and 0.63 for Th are obtained, supporting that the description by the model is reasonable. In case of the pyramidal $M(H_2S)^{4+}$ systems there are two M-SH_2 interactions of different size yielding $|v|/\Delta$ values of 0.27 and 6.60 for Ce and

0.28 and 1.19 for Th. Again, the higher covalency of the Ce system is confirmed by the Wiberg bond orders of 1.22 for Ce and 1.09 for Th. The corresponding values obtained from the model are 1.27 for Ce and 1.15 for Th, again in reasonable agreement with the results obtained from the full calculation. The higher covalency of $M(H_2S)^{4+}$ compared to $M(H_2O)^{4+}$ is reflected by the strong increase of the highest $|v|/\Delta$ values.

Table 1. Mulliken charges and orbital populations for s, p, d, f and g symmetries on the metal center of $M(H_2O)_n^{4+}$ $(n = 8,9)$ complexes. The populations of the closed shell M^{4+} cations have been subtracted from the orbital populations. Contributions of the nf, (n+1)f and (n+2)f orbitals (Ce n=4, Th n=5) to the f population (%). All values in a.u..

	Mulliken								
	Q(M)	s	p	D	f	g	nf	(n+1)f	(n+2)f
$Ce(H_2O)_8^{4+}$	2.474	0.199	0.117	0.823	0.332	0.053	48%	33%	18%
$Ce(H_2O)_9^{4+}$	2.501	0.214	0.093	0.811	0.325	0.056	47%	34%	16%
$Th(H_2O)_8^{4+}$	2.668	0.210	0.077	0.624	0.412	0.009	68%	29%	1%
$Th(H_2O)_9^{4+}$	2.664	0.225	0.064	0.638	0.399	0.009	67%	29%	1%

Table 2. Ahlrichs shared electron number SEN, Wiberg bond order, $|v|/\Delta$ and electron density at the Bader bond critical point $\rho(\vec{r}_c)$ for M-O interactions of $M(H_2O)_n^{4+}$ $(n = 8,9)$ complexes. All values in a.u..

	Ahlrichs SEN	Wiberg BO	This work $\lvert v\rvert/\Delta$	Bader $\rho(\vec{r}_c)$	Bader $\nabla^2\rho(\vec{r}_c)$
$Ce(H_2O)_8^{4+}$	0.322	0.305	0.432	0.0601	0.022
$Ce(H_2O)_9^{4+}$	0.270,0.315	0.270,0.278	0.402,0.414	0.0555,0.0537	0.020,0.021
$Th(H_2O)_8^{4+}$	0.303	0.300	0.426	0.0535	0.019
$Th(H_2O)_9^{4+}$	0.237,0.315	0.282,0.289	0.407,0.422	0.0478,0.0493	0.017,0.018

As a more realistic example we chose the hydration complexes $M(H_2O)_n^{4+}$ $(n = 8,9)$ of tetravalent Ce and Th ions with eight- and nine-fold coordination of water molecules as test systems. The underlying electronic structure calculations [41] were performed at the HF level using relativistic pseudopotentials for the metals [36, 37]. Basis sets of quadruple-zeta quality were applied [38, 39]. Selected parameters characterizing the bonding were calculated and are summarized in Tables 1 and 2. These descriptors are useful to determine the type of bonding, but none of them can be related in a strict way to the overall strength of bonding. Coupled-cluster calculations with singles, doubles and perturbative triples (CCSD(T)) using AVTZ basis sets find in gasphase for both eight- and nine-fold coordination the Ce complexes (D_e 3506, 3673 kJ/mol) to be by about 9-10% more stable than the Th ones (D_e 3183, 3361 kJ/mol) [41]. The Gibbs energies of hydration derived from these results agree very well with experimental data.

The HF gasphase binding energies (Ce 3505, 3722 kJ/mol, Th 3208, 3424 kJ/mol) follow the same trend as the CCSD(T) results. A Mulliken population analysis of the HF density matrices yields about 7% higher charges on Th than on Ce, i.e., the Ce complexes are more covalent, cf. Table 1. The largest contributions in accepting density from the water ligands stem from the d (Ce 54%, Th 47%) and f (Ce 22%, Th 30%) orbitals. Further contributions arise from the s (Ce 13%, Th (16%), p (Ce 7%, Th 5%) and g (Ce 4%, Th 1%) orbitals. Since generalized contracted atomic natural orbital (ANO) basis sets were applied the contributions of individual shells can be identified. Whereas for the s, p and d symmetries the contributions arise almost completely from the lowest unoccupied orbitals of the M^{4+} ions, higher virtual f orbitals contribute to about 50% for Ce and 30% for Th, implying that quite flexible basis sets have to be used in order to capture f covalency.

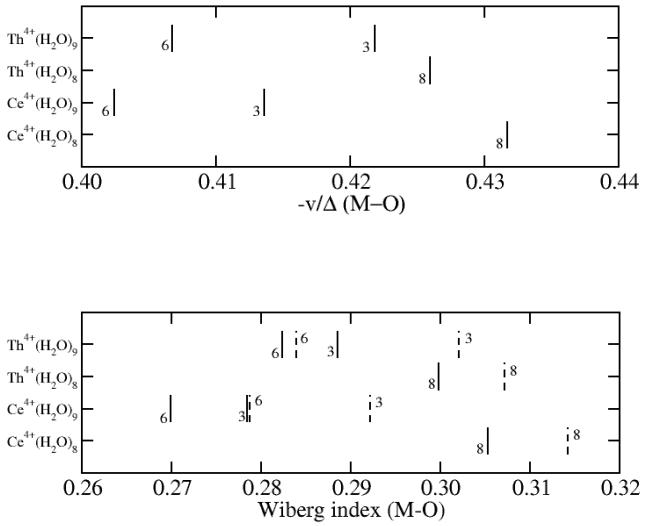

Figure 8. Bonding analysis for tetravalent Ce and Th hydration complexes $M(H_2O)_n^{4+}$ $(n = 8,9)$. Top: $|v|/\Delta$. Bottom: Wiberg bond order. The solid bars correspond to values extracted for the full calculation, whereas the dashed bars to those calculated with the model. For both plots the number of O atoms for each value is denoted at the bars.

The shared electron number proposed by Ahlrichs and coworkers [42] as well as the density at the bond critical point advocated by Bader [32] also indicate that the Ce complexes are slightly more covalent than the Th ones. Both schemes also suggest that the covalency is somewhat higher for the eight-fold coordination than the nine-fold one, probably due to the ≈0.03-0.05Å longer M-O distances and the associated smaller overlap and interaction for the latter systems. The low values of $\rho(\vec{r}_c)$ as well as the positive values of $\nabla^2\rho(\vec{r}_c)$ indicate a dominant ionic bonding.

The analysis using the two-electron two-orbital model described above does not yield a completely agreeing picture. Typically one localized orbital per free electron pair of the water molecules is found to contribute, i.e., one has $2n$ interactions to analyze in a $M(H_2O)_n^{4+}$ $(n = 8,9)$ complex. Since it is not necessary to provide the full picture with the limiting curves, only the $|v|/\Delta$ values, summed over pairs of atoms, are reported in Figure 8, top. By comparing the magnitude of the $|v|/\Delta$ values for the Ce and Th hydration complexes with, e.g., Figure 6, it is obvious that the bonding is essentially ionic with only small covalent contributions. Such small contributions, however, are important, e.g., they play a role for the selectivity of chelating agents used in the separation of lanthanide and actinide ions [43]. The Ce and Th hydration complexes belong to case 1 discussed above, i.e., when the weak interaction $|v| << \Delta$ is increased, the covalency and the stability increase, as can be seen for the change from nine- to eightfold coordination (shorter M-O distances, larger overlap, larger interaction) and the binding energies per H_2O molecule. Case 2 systems were subject of a previous publication [30]. The M-O covalency estimated using eqn. 10 is almost identical for Ce 8.2% and Th 8.0% for the $M(H_2O)_8^{4+}$ complexes (O_8 quadratic antiprisma), as well as for Ce 7.6%, 7.2% and Th 7.9%, 7.4% for the $M(H_2O)_9^{4+}$ complexes (O_9 tricapped trigonal prisma), i.e., the differences are quite small. In agreement with other methods for a given metal ion the nine-fold coordination is less covalent than the eight-fold one, and the Ce complex is more covalent than the one with Th, however this order is reversed for the nine-fold coordination.

That the findings for $|v|/\Delta$ are not unreasonable can be shown, e.g., by a comparison to the Wiberg bond orders [40], depicted in Figure 8, bottom (solid bars), which essentially give the same results as $|v|/\Delta$. Note that for a single bond $|v|/\Delta$ ranges from zero to infinity, whereas the Wiberg bond order is bounded by zero and one. When extracting as a check the Wiberg indices from the two-electron two-orbital model (dashed bars) these typically agree within 5% or better with those resulting from the full calculation, unless the mapping is poor due to orbitals not well localized between the metal center and the coordinating ligand atoms.

Applying the model in a predictive fashion is more involved, especially the determination of 'reasonable' orbital energies or matrix elements F_{MM} and F_{LL} of the fragments is not straightforward. We performed HF calculations using the MOLPRO program system [44, 45] for the separated M^{4+} ions and the surrounding n H_2O molecules. Note that at the HF level the lowest unoccupied orbitals of M^{4+} are at a lower energy than the highest occupied orbitals of H_2O, so that Δ values with a wrong sign would result. Since the metal-ligand interaction involves primarily a donation of electron density from lone-pairs of the ligand to the empty orbitals on the metal, we determined Δ as follows. By adding an electron pair to specific frozen virtual orbitals (M nf, (n+1)f, (n+1)d, (n+2)d, (n+2)p, (n+3)p, (n+2)s, (n+3)s, Ce n=4, Th n=5) of the M^{4+} ions (electron pair acceptors), and dividing the difference of the total energies of M^{2+} and M^{4+} by two, it is possible to derive effective one-electron energies corresponding to F_{MM}. Removing an electron pair from the $4n$ localized valence orbitals of the n H_2O molecules (electron pair donors), and dividing the difference of the total energies of $(H_2O)_n$ and $(H_2O)_n^{2+}$ by two, leads to effective one-electron energies corresponding to F_{LL}. When using this prescription Δ has the expected sign and a reasonable magnitude.

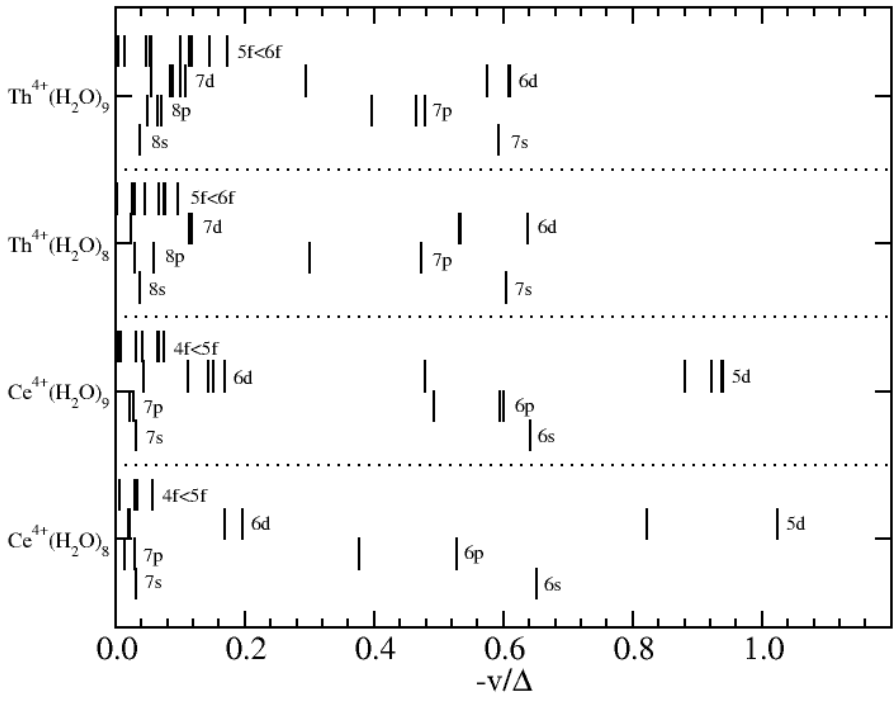

Figure 9. Estimated $|v|/\Delta$ values from separate calculations of M^{4+} and H_2O to predict Ce and Th orbital participation in bonding in $M(H_2O)_n^{4+}$ $(n = 8,9)$ complexes.

Overlap integals S_{LM} between the $(H_2O)_n$ ligand and the M^{4+} central ions were calculated with the Multiwfn code [46]. By applying the Wolfsberg-Helmholz formula [26] one can derive the parameter $|v|$, i.e., $v = F_{LM} = 1.75 * (F_{LL} + F_{MM}) * S_{LM}$. The energetic stabilisation ΔE for pairwise interactions between metal and ligand orbitals was estimated with eqn. 9. The sum of m pairwise interactions was then maximized under the condition that each orbital occurs only in one interacting pair, by applying an algorithm to solve a modified maximum-weighted matching problem. Hereby m is the minimum of the numbers of contributing fragment orbitals, i.e., usually the number of virtual orbitals on M^{4+} considered. For the selected pairs the $|v|/\Delta$ values were calculated and plotted in Figure 9. It is seen that the Ln 5d and An 6d orbitals by far are most likely to undergo covalent interactions with the ligand orbitals. The Ce complexes are expected to have more covalent contributions than the Th complexes. The Ce 6s, 6p and Th 7s, 7p orbitals should also contribute to the covalency. Interestingly, for the f symmetry the Ce 5f and Th 6f orbitals are more suitable for covalent interactions than the actual Ce 4f and Th 5f valence orbitals, implying that in actual calculations flexible f basis sets have to be applied in order to capture f orbital covalency. This is mainly due to the larger overlap integrals of the (n+1)f shells compared to the nf ones, which is not compensated by a larger energy gap Δ, leading ultimately to a larger interactions $|v|$. For the s and p symmetries the (n+3)s and (n+3)p orbitals have both smaller overlap and a larger energy gap than (n+2)s and (n+2)p, so that only the latter play a role. The overlap integrals of (n+2)d are also somewhat larger than those of (n+1)d, but a much larger energy gap for (n+2)d results in the dominant role of the (n+1)d shells. Due to symmetry reasons four of the five d orbitals contribute much more than the fifth one. Quantitatively these 'predictions' based on fragment calculations are in line with the 'analysis' of the full calculations of the complexes outlined above, except for one aspect, i.e., $Ce(H_2O)_9^{4+}$ is expected to have more covalency than $Th(H_2O)_9^{4+}$ from calculations of the fragments, whereas it has less on the basis of calculations of the complexes. Nevertheless, a qualitatively correct picture showing which orbitals are likey to contribute to covalent interactions is provided. In summary the model appears to describe bonding in mainly ionic metal complexes sufficiently correct to support the findings at the beginning of the article concerning the two types of covalency discussed in literature.

4. Conclusion

A simple two-electron two-orbital textbook model for chemical bonding was summarized and used to analyze ionic and covalent bonding contributions in metal complexes. The model works with parameters familiar from simple molecular orbital diagrams. It can explain, e.g., both the increase and the decrease of bond strength upon strengthening the covalent character of the bond. In particular, the region of the often postulated energy (near-)degeneracy driven covalency in actinide-ligand bonds is associated with the case of ordinary weak covalent bonding with small ionic contributions. It was shown that the model can be used to analyze metal-ligand interactions by extracting information from HF or KS calculations as well as to predict the contribution of metal orbitals in such interactions on the basis of calculations for the fragments.

Acknowledgements

Support by the NSFC under grant number W2441007 is gratefully acknowledged. The author is also grateful to a reviewer for several valuable hints.

References

[1] Diamond R.M., Street Jr. K., Seaborg G.T. An ion-exchange study of possible hybridized 5f bonding in the actinides. *J. Am. Chem. Soc.*, **76** (1954), 1461-1469.

[2] Bursten B.E., Strittmatter R.J. Cyclopentadienyl-actinide complexes: bonding and electronic structure. *Angew. Chem. Int. Ed. Engl.*, **30** (1991), 1069-1085.

[3] Pepper M., Bursten B.E. The electronic structure of actinide-containing molecules: a challenge to applied quantum chemistry. *Chem. Rev.*, **91** (1991), 719-741.

[4] Denning R.G. Electronic structure and bonding in actinyl ions. *Struct. Bond.*, **79** (1992), 215-276.

[5] Dolg M. In: *Encyclopedia of Computational Chemistry*, eds.: P. v. R. Schleyer, N. L. Allinger, T. Clark, J. Gasteiger, P. A. Kollman, H. F. Schaefer III, P. R. Schreiner, Wiley, Chichester, 1998, pp. 1478-1486.

[6] Schreckenbach G., Hay P.J., Martin R.L. Density functional calculations on actinide compounds: survey of recent progress and application to $[UO_2X_4]^{2-}$ (X = F, Cl, OH) and AnF_6 (An = U, Np, Pu). *J. Comput. Chem.*, **20** (1999), 70-90.

[7] Matsika S., Zhang Z., Brozell S.R., Blaudeau J.P., Wang Q., Pitzer R.M. Electronic structure and spectra of actinyl ions. *J. Phys. Chem. A*, **105** (2001), 3825-3828.

[8] Dolg M., Cao X. In: *Computational Inorganic and Bioinorganic Chemistry*, eds.: E. I. Solomon, R. A. Scott, R. B. King, Wiley, Chichester, 2009, pp. 503-515.

[9] Kaltsoyannis N. Does covalency increase or decrease across the actinide series? Implications for minor actinide partitioning. *Inorg. Chem.*, **52** (2013), 3407-3413.

[10] Dognon J.-P. Electronic structure theory to decipher the chemical bonding in actinide systems. *Coord. Chem. Rev.*, **344** (2017), 150-162.

[11] Kerridge A. Quantification of f-element covalency through analysis of the electron density: insights from simulation. *Chem. Commun.*, **53** (2017), 6685-6695.

[12] Dolg M., Cao X. In: *Encyclopedia of Inorganic and Bioinorganic Chemistry*, *The Heaviest Metals: Science and Technology of the Actinides and Beyond*, eds.: T. P. Hanussa, W. Evans, Wiley, Chichester, 2018, DOI: 10.1002/9781119951438.eibc2540.

[13] Kaltsoyannis N. Transuranic computational chemistry. *Chem. Eur. J.*, **24** (2018), 2815-2825.

[14] Pace K.A., Klepov V.V., Berseneva A.A., zur Loye H.-C. Covalency in actinide compounds. *Chem. Eur. J.*, **27** (2021), 5835-5841.

[15] Kaltsoyannis N., Kerridge A. Understanding covalency in molecular f-block compounds from the synergy of spectroscopy and quantum chemistry. *Nature Rev. Chem.*, **8** (2024), 701-712.

[16] Neidig M.L., Clark D.L., Martin R.L. Covalency in f-element complexes. *Coord. Chem. Rev.*, **257** (2013), 394-406.

[17] Minasian S.G., Keith J.M., Batista E.R., Boland K.S., Clark

D.L., Conradson S.D., Kozimor S.A., Martin R.L., Schwarz D.E., Shuh D.K., Wagner G.L., Wilkerson M.P., Wolfsberg L.E., Yang P. Determining relative f and d orbital contributions to M–Cl covalency in MCl_6^{2-} (M = Ti, Zr, Hf, U) and $UOCl_5^-$ using Cl K-edge X-ray absorption spectroscopy and time-dependent density functional theory. *J. Am. Chem. Soc.*, **134** (2012), 5586-5597.

[18] Spencer L.P., Yang P., Minasian S.G., Jilek R.E., Batista E.R., Boland K.S., Boncella J.M., Conradson S.D., Clark D.L., Hayton T.W., Kozimor S.A., Martin R.L., MacInnes M.M., Olson A.C., Scott B.L., Shuh D.K., Wilkerson M.P. Tetrahalide complexes of the $[U(NR)_2]^{2+}$ ion: synthesis, theory, and chlorine K-edge X-ray absorption spectroscopy. *J. Am. Chem. Soc.*, **135** (2013), 2279-2290.

[19] Minasian S.G., Keith J.M., Batista E.R., Boland K.S., Clark D.L., Kozimor S.A., Martin R.L., Shuh D.K., Tyliszczak T. New evidence for 5f covalency in actinocenes determined from carbon K-edge XAS and electronic structure theory. *Chem. Sci.*, **5** (2014), 351-359.

[20] Cross J.N., Su J., Batista E.R., Cary S.K., Evans W.J., Kozimor S.A., Mocko V., Scott B.L., Stein B.W., Windorff C.J., Yang P. Covalency in americium(III) hexachloride. *J. Am. Chem. Soc.*, **139** (2017), 8667-8677.

[21] Kelley M.P., Su J., Urban M., Luckey M., Batista E.R., Yang P., Shafer J.C. On the origin of covalent bonding in heavy actinides. *J. Am. Chem. Soc.*, **139** (2017), 9901-9908.

[22] Vitova T., Pidchenko I., Fellhauer D., Bagus P.S., Joly Y., Pruessmann T., Bahl S., Gonzalez-Robles E., Rothe J., Altmaier M., Denecke M.A., Geckeis H. The role of the 5f valence orbitals of early actinides in chemical bonding. *Nat. Commun.*, **8** (2017), 16053.

[23] Su J., Batista E.R., Boland K.S., Bone S.E., Bradley J.A., Cary S.K., Clark D.L., Conradson S.D., Ditter A.S., Kaltsoyannis N., Keith J.M., Kerridge A., Kozimor S.A., Löble M.W., Martin R.L., Minasian S.G., Mocko V., La Pierre H.S., Seidler G.T., Shuh D.K., Wilkerson M.P., Wolfsberg L.E., Yang P. Energy-degeneracy-driven covalency in actinide bonding. *J. Am. Chem. Soc.*, **140** (2018), 17977-17984.

[24] Platts J.A., Baker R.J. A computational investigation of orbital overlap versus energy degeneracy covalency in $[UE_2]^{2+}$ (E = O, S, Se, Te) complexes. *Dalton Trans.*, **49** (2020), 1077-1088.

[25] Pereiro F.A., Galley S.S., Jackson J.A., Shafer J.C. Contemporary assessment of energy degeneracy in orbital mixing with tetravalent f-block compounds. *Inorg. Chem.*, **63** (2024), 9687-9700.

[26] Wolfsberg M., Helmholz L. The spectra and atomic structure of the tetrahedral ions MnO_4^-, CrO_4^-, and ClO_4^-. *J. Chem. Phys.*, **20** (1952), 837-843.

[27] Sergentu D.-C., Autschbach J. Covalency in actinide(iv) hexachlorides in relation to the chlorine K-edge X-ray absorption structure. *Chem. Sci.*, **13** (2022), 3194-3207.

[28] Smith P.W., Sergentu D.-C., Branson J.A., Peterson A., Russo D.R., Booth C.H., Autschbach J., Minasien S.G. X-ray spectroscopy of $CeBr_6^{2-}$ and comparisons to the corresponding chloride and fluoride complexes. *ChemRxiv*, (2025), DOI: 10.26434/chemrxiv-2025-3rn19.

[29] Sergentu D.-C., Duignan T.J., Autschbach J. *Ab initio* study of covalency in the ground versus core-excited states and X-ray absorption spectra of actinide complexes. *J. Phys. Chem. Lett.*, **8** (2018), 5583-5591.

[30] Sadhu B., Dolg M. Enhancing actinide(iii) over lanthanide(iii) selectivity through hard-by-soft donor substitution: exploitation and implication of near-degeneracy-driven covalency. *Inorg. Chem.*, **58** (2019), 9738-9748.

[31] Ji W.-X., Xu W., Schwarz W.H.E., Wang S.-G. Ionic bonding of lanthanides, as influenced by d- and f-atomic orbitals, by core-shells and by relativity. *J. Comput. Chem.*, **36** (2015), 449-458.

[32] Bader R.F.W. *Atoms in Molecules. A Quantum Theory.*, Oxford University Press, Oxford, UK, 1990.

[33] Nordholm S., Bacskay G.B. The basics of covalent bonding in terms of energy and dynamics. *Molecules*, **25** (2020), 2667.

[34] *TURBOMOLE*, version 7.5, program package developed by the Quantum Chemistry Group, University of Karlsruhe and Forschungszentrum Karlsruhe GmbH 1989-2007; TURBOMOLE GmbH, Karlsruhe, since 2007. URL: https://www.turbomole.org.

[35] Balasubramani S.G., Chen G.P., Coriani S., Diedenhofen M., Frank M.S., Franzke Y.J., Furche F., Grotjahn R., Harding M.E., Hättig C., Hellweg A., Helmich-Paris B., Holzer C., Huniar U., Kaupp M., Khah A.M., Khani S.K., Müller T., Mack F., Nguyen B.D., Parker S.M., Perlt E., Rappoport D., Reiter K., Roy S., Rückert M., Schmitz G., Sierka M., Tapavicza E., Tew D.P., van Wüllen C., Voora V.K., Weigend F., Wodyński A., Yu J.M. Turbomole: modular program suite for *ab initio* quantum chemical and condensed-matter simulations. *J. Chem. Phys.*, **152** (2020), 184107.

[36] Dolg M., Stoll H., Preuß H. Energy-adjusted *ab initio* pseudopotentials for the rare earth elements. *J. Chem. Phys.*, **90** (1989), 1730-1734.

[37] Küchle W., Dolg M., Stoll H., Preuß H. Energy-adjusted pseudopotentials for the actinides. Parameter sets and test calculations for thorium and thorium monoxide. *J. Chem. Phys.*, **100** (1994), 7535-7542.

[38] Cao X., Dolg M. Valence basis sets for relativistic energy-consistent small-core lanthanide pseudopotentials. *J. Chem. Phys.*, **115** (2001), 7348-7355.

[39] Cao X., Dolg M., Stoll H. Valence basis sets for relativistic energy-consistent small-core actinide pseudopotentials. *J. Chem. Phys.*, **118** (2003), 487-496.

[40] Wiberg K.B. Application of the Pople-Santry-Segal CNDO method to the cyclopropylcarbinyl and cyclobuyl cation and to bicyclobutane. *Tetrahedron*, **24** (1968), 1083-1096.

[41] Cao X., Dolg M. In preparation.

[42] Ehrhardt C., Ahlrichs R. Population analysis based on occupation numbers II. Relationship between shared electron numbers and bond energies and characterization of hypervalent contributions. *Theor. Chim. Acta*, **68** (1985), 231-245.

[43] Cao X., Heidelberg D., Ciupka J., Dolg M. First-principles study of the separation of Am III/Cm III from Eu III with Cyanex301. *Inorg. Chem.*, **49** (2010), 10307-10315.

[44] *Molpro*, version 2012.1, a package of *ab initio* programs, H.-J. Werner, P. J. Knowles, G. Knizia, F. R. Manby, M. Schütz et al., URL: http://www.molpro.net.

[45] Werner H.-J., Knowles P.J., Knizia G., Manby F.R., Schütz M. Molpro: a general-purpose quantum chemistry program package. *WIREs Comput. Mol. Sci.*, **2** (2012), 242-253.

[46] Lu T., Chen F. Multiwfn: a multifunctional wavefunction analyzer. *J. Comput. Chem.*, **33** (2012), 580-592.